Tributyltin (TBT) biodegradation induces oxidative stress of *Cunninghamella echinulata*

Adrian Soboń, Rafał Szewczyk, Jerzy Długoński

Department of Industrial Microbiology and Biotechnology, Institute of Microbiology, Biotechnology and Immunology, Faculty of Biology and Environmental Protection, University of Łódź, Banacha 12/16, 90-237 Łódź, Poland

Citation: Soboń A., Szewczyk R., Długoński J. Tributyltin (TBT) biodegradation induces oxidative stress of *Cunninghamella echinulata*. International Biodeterioration & Biodegradation (2016) 107:92-101
http://dx.doi.org/10.1016/j.ibiod.2015.11.013

Keywords: fungi; tributyltin; biodegradation; LC-MS/MS; proteomics; oxidative stress

Highlights

- Efficient TBT biodegradation to DBT, MBT and tin-hydroxylated byproduct was observed.
- TBT changed the protein and free amino acid profile.
- Markers of oxidative stress were upregulated in the presence of TBT.

Abstract

Tributyltin (TBT) is one of the most deleterious compounds introduced into natural environment by humans. The ability of *Cunninghamella echinulata* to degrade tributyltin (TBT) (5 mg l^{-1}) as well as the effect of the xenobiotic on fungal amino acids composition and proteins profile were examined. *C. echinulata* removed 91% of the initial biocide concentration and formed less hazardous compounds dibutyltin (DBT) and monobutyltin (MBT). Moreover, the fungus produced a hydroxylated metabolite (TBTOH), in which the hydroxyl group was bound directly to the tin atom. Proteomics analysis showed that in the presence of TBT, the abundances of 22 protein bands were changed and the unique overexpressions of peroxiredoxin and nuclease enzymes were observed. Determination of free amino acids showed significant changes in the amounts of 19 from 23 detected metabolites. A parallel increase in the level of selected amino acids such as betaine, alanine, aminoisobutyrate or proline and peroxiredoxin enzyme in TBT-containing cultures revealed that TBT induced oxidative stress in the examined fungus.

1. Introduction

Endocrine-disrupting compounds (EDCs) are a large group of exogenous chemicals that cause adverse health effects in numerous organisms. The receptor affinity mentioned here is mainly due to hormonal mimicry (Tabb and Blumberg 2006). A highly hazardous representative of this group is tributyltin (TBT), used for many years as a biocide in the textile industry and as an antifoulant agent in marine paints (Antizar-Ladislao 2008; Cruz et al. 2007). TBT demonstrates several cytotoxic properties on bacteria and higher living organisms (Liu, 2006; Gupta et al. 2011; Cruz et al. 2015). The presence of the toxic compounds in the environment induces changes in the cell structure and metabolism. A special role is played by the overproduction of reactive oxygen species (ROS), which cause extensive oxidation damage to numerous biomolecules including DNA, proteins and lipids. The ROS-originated damage may lead to cellular dysfunctions or even cell death (Ishihara et al. 2012), but the cells may fight with the high level of ROS with the use of enzymatic or non-enzymatic mechanisms. The first components of self-defence are antioxidant enzymes like superoxide dismutase (SOD), catalase (CAT) or guaiacol peroxidase (GPX). The other antioxidants involved in the cellular elements protection include: ascorbic acid, reduced glutathione, α-tocopherol, carotenoids, flavonoids and selected amino acids such as betaine or proline (Das and Roychoudhury 2014). However, the nature of molecular response against stress factors induced by organotin compounds remains poorly characterized. Studies conducted on *Cunninghamella elegans* as a eukaryotic model revealed a number of negative effects of TBT on the organism, such as changes in the lipid profile, increased potassium retention and disturbances in the hyphae morphology (Bernat et al. 2009b; Bernat and Długoński 2012; Bernat et al. 2014a).
Proteomics and metabolomics are useful tools for the research on the processes occurring in the cell leading to a deeper and more complex understanding of the cell behaviour under various stress or physiological conditions (Baxter and al. 2007; Bundy et al. 2009; Kroll et al. 2014). The current work was focused on the examination of the influence of TBT biodegradation on the amino acids composition and proteome expression of *Cunninghamella echinulata*, and revealed a significant upregulation of oxidative stress biomarkers .

2. Materials and methods

2.1. Chemicals

Tributyltin (TBT), dibutyltin (DBT), monobutyltin (MBT), tetrabutyltin (TTBT) and tropolone were purchased from Sigma-Aldrich (Germany). All other chemicals and ingredients used in the GC-MS and LC-MS/MS analysis and protein sample preparation were of high purity grade and were obtained from Sigma-Aldrich (Germany), Serva (Germany), Bio-Rad (USA), Avantor (Poland), or Promega (USA).

2.2. Strain and growth conditions

C. echinulata IM 2611 from the fungal collection of the Department of Industrial Microbiology and Biotechnology, University of Łódź, Poland, was the subject of the work. Spores originating from 10-day-old cultures on ZT slants (Bernat et al. 2013) were used to inoculate 20 ml of Sabouraud dextrose broth medium (Difco) supplemented with 2% glucose. The incubation was conducted in a 100-ml Erlenmeyer flask with a wide neck at 28°C on a rotary shaker (160 rpm). After 24 h, the precultures were transferred to fresh Sabouraud dextrose broth medium (in the ratio 1:4) and incubated for another 24 h in the same conditions as above. Two millilitres of the homogenous preculture was introduced into 18 ml of fresh Sabouraud dextrose broth medium (in a 100-ml Erlenmeyer flask with a wide neck) supplemented with TBT at 5 mg l^{-1} (TBT stock solution 5 mg ml^{-1} in ethanol) or without the xenobiotic as a biotic control. Additionally, an abiotic control of TBT (without the microorganism) was prepared. The cultures and controls were incubated for 5 days in the same conditions as described above. All samples were prepared in triplicate.

2.3. Butyltin determination

The organotins analysis was conducted according to the modified procedure described by Bernat and Długoński (2009a). The sample was acidified (pH 2) and homogenized using a mixer mill (Retsch MM400) with glass beads Ø1 mm for 5 min at 30 Hz. Next, the sample was extracted twice using a 20 ml mixture of 0.05% tropolone in hexane, dried over anhydrous Na_2SO_4 and evaporated. The extract was dissolved in 2 ml of hexane and derivatized by adding 0.5 ml of a Grignard reagent. The reaction was carried out in darkness at room temperature for 20 min. Next, the process was quenched by slow addition of cooled, 20% NH_4Cl (2 ml). The sample was next centrifuged at 3000 *g* for 10 min and the supernatant was analyzed. The butyltin determination was conducted using an Agilent 7890 gas chromatograph coupled with an Agilent 5975C mass detector. The separation was performed using an Agilent HP-5MS capillary column (30 m x 0.25 mm id. x 0.25 µm film thickness). The injection volume was set to 1.6 µl. The inlet was set to a split mode with a split ratio 10:1 and the temperature maintained at 280°C. Helium was used as a carrier gas. The column temperature parameters were as follows: 60°C maintained for 4 min, then

increased at 20°C min^{-1} ratio to 280°C and maintained for 3 min. Ions 165 m/z (for MBT), 151 m/z (DBT) and 193 m/z (TBT) were chosen for targeted quantitative analysis.

2.4. Sample preparation for LC-MS/MS analysis of TBT intermediates

The cultures were homogenized using a mixer mill (Retsch MM 400) with glass beads Ø1 mm for 5 min at 30 Hz. The analytes were extracted according to the modified QuEChERS protocol (available online at http://quechers.cvua-stuttgart.de). A 10-ml sample of the homogenate was mixed with 10 ml of ACN in a 50-ml centrifuge tube and was vortexed for 1 min. Next, 4 g of magnesium sulphate anhydrous, 1 g of sodium chloride, 1 g of trisodium citrate dihydrate and 0.5 g of disodium hydrogencitrate sesquihydrate were added, and the sample was vortexed for another 1 min. The samples were centrifuged for 3 min at 5000 *g,* and the supernatant was analysed by LC-MS/MS. All samples were prepared in triplicate.

2.5. Sample preparation for amino acids analysis

The sample preparation was performed according to the procedure described by Szewczyk et al. (2015). Mycelium (100 mg) was placed into 2-ml Eppendorf tubes containing 1 ml of cold water and homogenized with a cold glass matrix Ø1 mm on FastPrep-24 (MP Biomedicals, USA) three times for 30 s at a velocity 4 m s^{-1} using a 2 min break between each homogenization in order to cool the sample; the sample was then centrifuged at 4000 *g* at 4°C for 10 min. Supernatant (100 µl) was vortexed with 900 µl 0.1% formic acid in ethanol for 3 min and incubated for 2 h at -20°C. Next, the sample was centrifuged at 14000 *g* for 20 min at 4°C and the supernatant was collected into a separate 1.5-ml Eppendorf tube and evaporated at 30°C under a vacuum. Dry extracts were stored at -70°C for further analysis. The content of a frozen sample was resuspended in 1 ml of 2% ACN in water, sonicated and vortexed for 2 min, and incubated for 1 h at 4°C. Finally, the samples were diluted 20-times prior to LC-MS/MS analysis.

2.6. LC-MS/MS analysis of TBT metabolites

LightSight™ software was used to predict the multiple reaction monitoring (MRM) transitions for various phase I and II metabolites. Moreover, neutral loss and precursor ion scans for glucuronide and glutathione conjugates were performed. Qualitative analyses were performed using an Eksigent expert™ microLC200 chromatograph coupled with an AB Sciex QTRAP 4500 mass spectrometer. Chromatographic separation was conducted on a reverse-phase Eksigent C18-AQ (0.5 mm x 150 mm x 3 µm, 120 Å) column: temperature 40°C, injection volume: 5 µl. The applied eluents consisting of 2 mM of ammonium formate and 0.1% of formic acid in both water (A) and acetonitrile (B) were used. The gradient with a constant flow of 10 µl min^{-1} and 0.5 min preflush conditioning was as follows: started from 98% of eluent A for 0.2 min; 100% of eluent B after 15 min and maintained until 7 min; reversed to the initial conditions from 22.1-23 min. The optimized ESI ion source parameters were as follows: CUR: 25; IS: 5000 V; TEMP: 400°C; GS1: 20; GS2: 40; ihe: ON for the positive ionization mode and IS: -4500 V for the negative ionization mode, respectively. Several methods with different CE settings were tested (30±15 V; 50±15 V; 60±15 V), especially for phase II metabolites.

2.7. Amino acids analysis

The LC-MS/MS screening method in the MRM mode applied for investigation of the amino acids composition was based on a multi-method developed by Wei et al. (2010). An Eksigent expert™ microLC chromatograph coupled with an AB Sciex QTRAP 4500 mass spectrometer was employed for the analysis. Chromatographic separation was performed on a reverse-phase Eksigent ChromXP C8EP (0.5 x 150 mm x 3 µm, 120Å) column. The temperature was set to 35°C and the injection volume was set to 5 µl. The applied eluents were water with 0.1% of formic acid (A) and acetonitrile with 0.1% of formic acid. (B). The gradient with a constant flow of 50 µl min^{-1} and 0.5 min preflush conditioning was as follows: start from 98% of eluent A for 0.2 min; 90% of eluent B after 2.2 min and maintained to 3.4 min; reversed to the initial conditions from 4 min. The positive ionization ESI ion source parameters were as follows: CUR: 25; IS: 5000 V; TEMP: 300°C; GS1 and GS2: 30; ihe: ON. The compound-dependent MRM parameters were presented in table S-1.

2.8. Protein extraction

Protein extraction was performed as described previously (Szewczyk et al. 2014). Mycelia (3.5±0.2 g) from the 5-day-old control and TBT-containing samples were separated from the culture media, transferred to a lytic buffer and mechanically homogenized using glass beads on a FastPrep-24 (MP Biomedicals, USA). Proteins were precipitated with 20% trichloroacetic acid and resuspended in an SSSB buffer (8 M urea, 4% w/v CHAPS, 1% w/v DTT). The total protein content was measured using the Bradford method with BSA (Sigma-Aldrich, Germany) as the protein standard. The samples were stored at -70°C for further use.

2.9. 1-D electrophoresis

The protein samples (10 µg) were separated on 12% mini gels (mini-Protean tetra cell, Bio-Rad) as described previously (Bernat et al. 2014b). The gels were stained with Coomassie blue, imaged using the ChemiDoc System (Bio-Rad) and analysed using the Image Lab v.4.1 (Bio-Rad).

2.10. Protein digestion

Protein digestion with trypsin was conducted according to the procedure described by Shevchenko et al. (2006). The selected protein bands were excised and placed into 0.5-ml LoBind tubes (Eppendorf). The gels were cut into approximately 1 x 1 mm fragments. Then, the reduction and acylation of proteins were performed. Next, the gels were saturated with trypsin (Sequencing Grade Modified Trypsin, Promega) and incubated overnight at 37°C. After digestion, peptides were extracted with 50 µl of 0.1% trifluoroacetic acid (TFA) solution in 2% ACN and analysed.

2.11. LC-MS/MS analysis of peptides

The LC-MS/MS analysis of digested proteins was performed using the Eksigent expert™ microLC 200 system coupled with a QTRAP 4500 (AB Sciex) (Bernat et al. 2014b). The 10 µl of peptides was injected onto a reversed-phase Eksigent C8CL-120 column (0.5 x 100 mm, 3µm) and separated for 53 min at 40°C. MS/MS analysis was operated in a data-dependent mode with optimized ESI parameters as follows: ion spray (IS) voltage of 5000 V, declustering potential of 100 V, and temperature of 300°C. The precursor ions range was chosen from *m/z* 500 to *m/z* 1500, and the product ions range was chosen from *m/z* 50 to *m/z* 2000. The ion source GS1, GS2 and CUR parameters were set at 20, 20, and 25, respectively.

2.12. Database search

The Protein Pilot v4.0 software (AB Sciex), coupled with the MASCOT search engine v2.3, was used for the database searches. The data were searched against the NCBI and Swiss-Prot+TrEMBL databases with taxonomy filtering set to fungi (ver. 04.2015, total number of fungi sequences 5566597 and 3479123, respectively). Mascot MS/MS ion searches were performed with trypsin chosen as a protein digesting enzyme, up to two missed cleavages were tolerated and the following variable modifications were applied: Acetyl (N-term), Carbamidomethyl (C), Deamidated (NQ), Formyl (N-term), Gln->pyro-Glu (N-term Q), Glu->pyro-Glu (N-term E), and Oxidation (M). Searches were conducted with a peptide mass tolerance of 1 Da and a fragment ion mass tolerance of 0.5 Da.

2.13. Statistical analysis

All experiments were prepared in triplicate. T-test was used to determine the significance of the differences between the samples. The data were considered as significant if $P < 0.05$. Principal component analysis (PCA) of the MRM data (chromatography peak areas and retention times) obtained from the microLC-MS/MS analysis was conducted with the MarkerView™ software (AB Sciex, USA). Pareto algorithm was applied for the PCA calculation. Statistical analysis and hit map presentation of the data obtained from PCA loadings were performed with the use of Excel 2007 (Microsoft Corporation, USA).

3. Results

3.1. TBT quantitative analysis

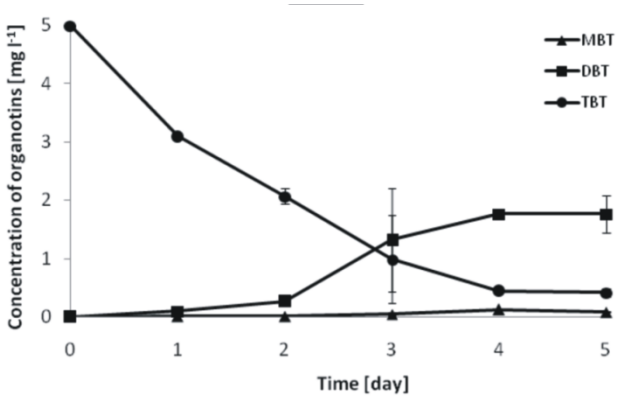

Fig. 1. TBT degradation by *C. echinulata* IM 2611 (*n*=3).

C. echinulata IM 2611 was capable of efficient TBT (5 mg l^{-1}) degradation to less toxic metabolites - DBT and MBT during 5 days of the culture (Fig. 1). After 5 days of incubation, fungus eliminated 91% of the initial xenobiotic concentration (0.42 mg l^{-1}) and transformed the substrate to DBT (1.77 mg l^{-1}) and MBT (0.08 mg l^{-1}). Moreover, TBT strongly inhibited the growth of the tested strain during the first 48 h of incubation (Fig. 2). Additionally, an increase in the concentration of degradation by-products was correlated with the fungus growth.

3.2. TBT qualitative analysis

The TBT fragmentation pattern had been described previously (Banoub et al. 2004; Békri et al. 2006). On the basis of the optimized product ions of TBT, the predicted MRM LC-MS/MS methods were developed using LightSight™ software and applied for the screening of possible metabolites. These methods included phase I, phase II and distinct GSH conjugates screening. Samples for qualitative analysis, including corresponding biotic and abiotic controls acting as a reference for TBT intermediates searching, were collected every 24 h during 5 days of the experiment.

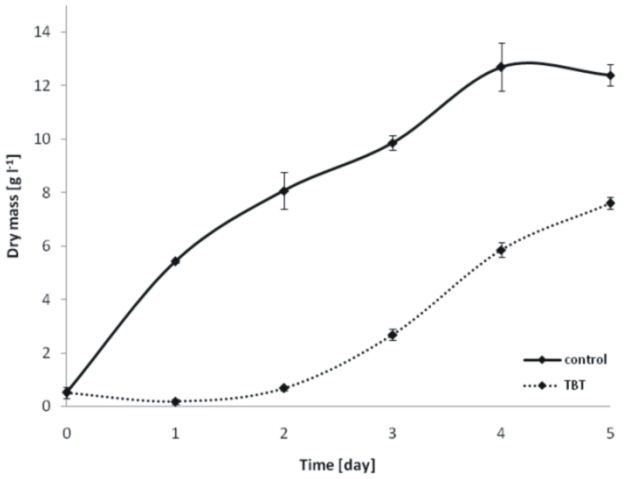

Fig. 2. Time course of growth of *C. echinulata* IM 2611 in the presence of TBT in concentration 5 mg l^{-1} (dotted lines) compared to the control samples (continuous lines) (*n*=3).

A novel TBT intermediate, tributyltin hydroxide (TBTOH) (Fig. 3C), was detected. The mass spectrum analysis of the 309 m/z, 307 m/z and 305 m/z tin isotopes (RT 10.6 min) showed that the hydroxyl group was attached directly to the tin atom. The characteristic 251 m/z ion was formed by the loss of one butyl group from TBTOH [M-C_4H_9]$^+$; the 233 m/z species were attributed to the loss of the butyl and the hydroxyl group [M-C_4H_9OH]$^+$, which gave the DBT ion; 195 m/z corresponded to an MBT ion coupled with the hydroxylated group; the 175-177 m/z ion was produced by the loss of another butyl and hydroxyl group [M-C_4H_9-C_4H_8OH]$^+$; the 137 m/z was attributed to the loss of the third butyl group from TBTOH [M-$C_{12}H_{26}$]$^+$; finally, the 16 Da mass shift between 137 and 121 m/z showed that the oxygen atom was bonded to the tin (Fig. 3C). Additionally, selected MS^3 experiments aimed at the characterization of a unique 195 m/z ion (and its tin isotopes) fragmentation pathway were performed to confirm the point of oxygen attachment (Fig. 3D). The LC-MS/MS analysis did not show any other TBT intermediates of phases I and II.

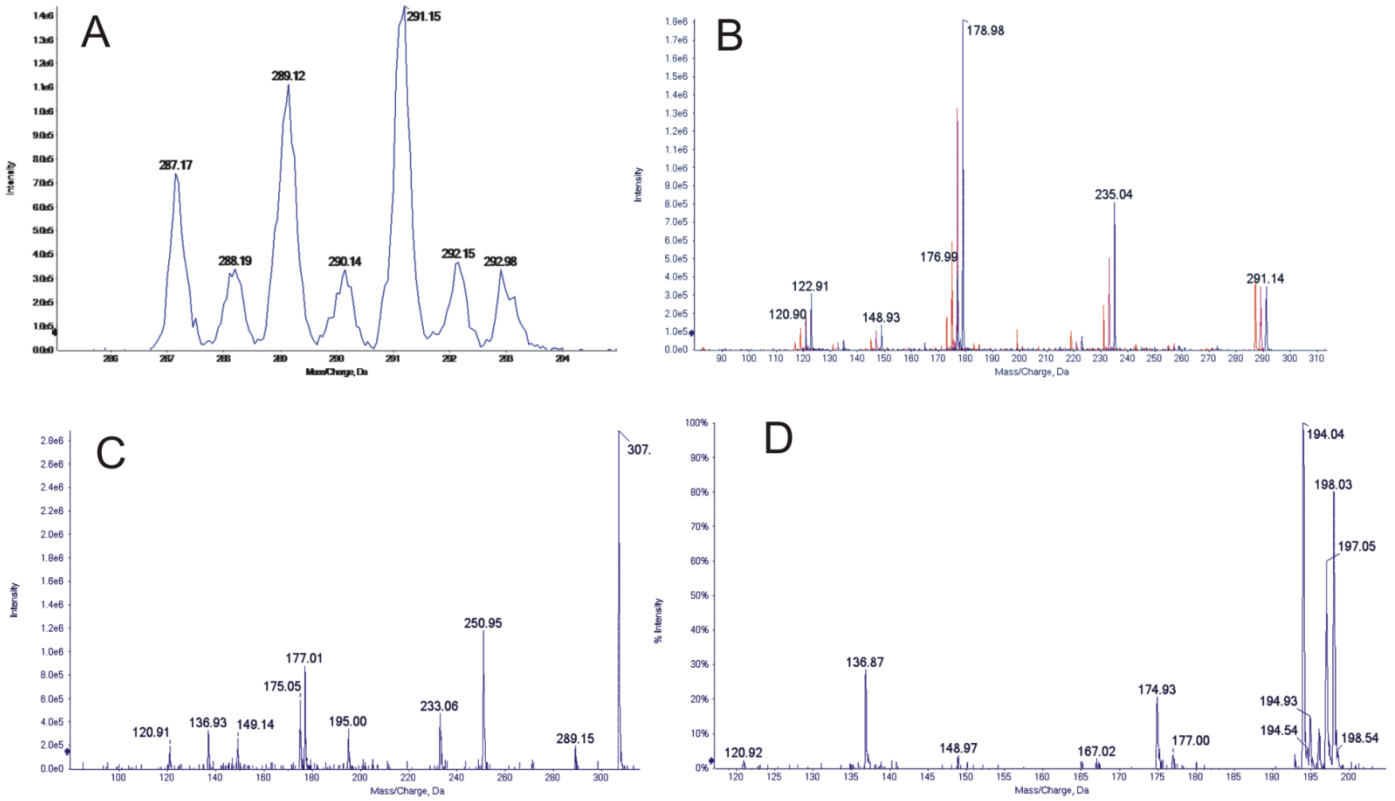

Fig. 3. Mass spectra and fragmentation patterns of TBT and novel, hydroxylated TBT intermediate (TBTOH). (A) ER scan of TBT; (B), fragmentation pattern of TBT (287, 289 and 291 m/z) containing characteristic tin isotopes: ^{116}Sn (orange), ^{118}Sn (purple) and ^{120}Sn (blue), respectively; (C) mass spectra of TBTOH (307 m/z) containing ^{118}Sn; (D) MS^3 experiment for 195 m/z originating from TBTOH (307 m/z).

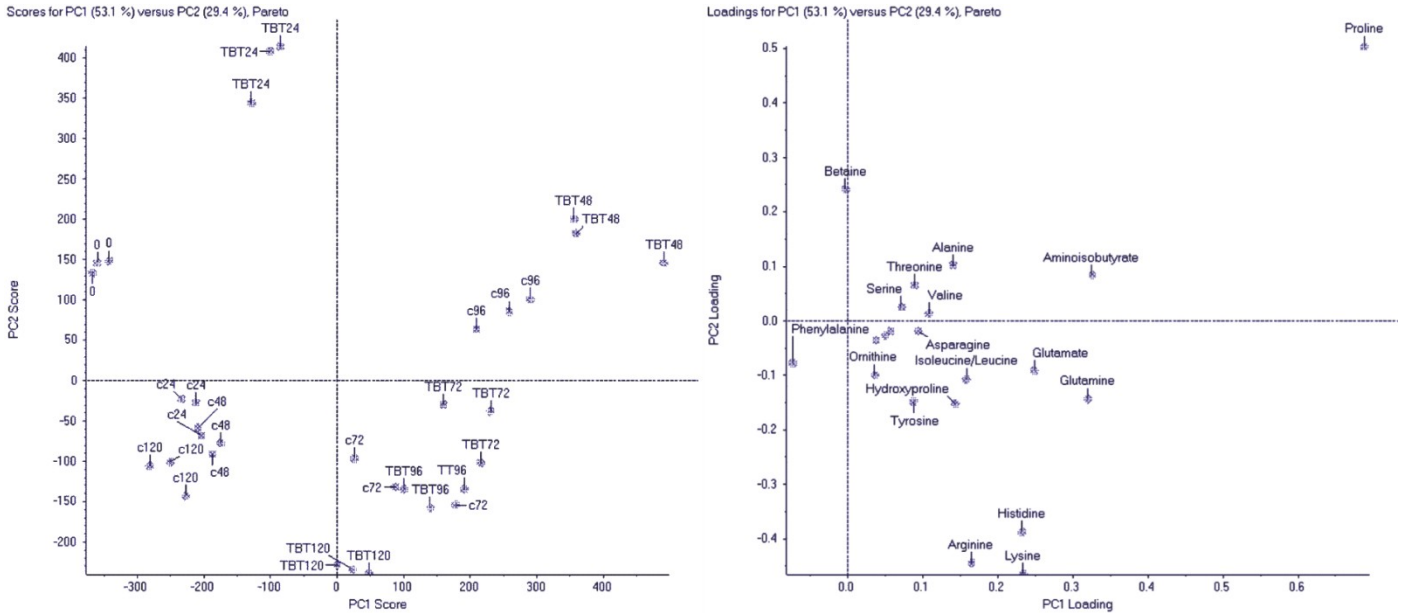

Fig. 4. PCA analysis of the mycelial amino acids metabolism on TBT-containing (5 mg l-1) and control cultures on Sabouraud medium. On the left – PC1 against PC2 loading charts; on the right – PC1 against PC2 scoring chart.

Table 1. Relative concentration of the monitored amino acids during TBT (5 mg l-1) biodegradation by *C. echinulata* IM 2611 on Sabouraud medium.

	Control culture						TBT containing culture				
Amino acid	0	24c	48c	72c	96c	120c	24TBT	48TBT	72TBT	96TBT	120TBT
Aminoisobutyrate[24,48]	13	29	33	63	69	35	72	100	80	74	57
Alanine[24,48,120]	26	31	40	79	64	27	99	100	72	75	49
Arginine[24,48,120]	11	36	49	81	70	57	4	31	71	90	100
Asparagine[48,72,96,120]	19	27	26	42	34	27	22	100	76	71	49
Aspartate[24,48,96,120]	26	31	30	67	100	26	20	51	42	42	53
Betaine[24,120]	12	9	14	13	16	6	100	24	12	13	10
Dimethyl glycine[24]	35	73	70	80	92	53	32	100	72	76	68
Glutamate[48,96,120]	6	14	17	81	100	10	26	51	47	55	72
Lysine[24,96]	23	67	84	93	74	79	4	89	100	100	99
Glutamine[24,48,72,120]	7	37	28	50	90	26	8	97	100	94	68
Histidine[24,96,120]	17	45	54	99	52	62	9	81	84	91	100
Hydroxyproline[48,72,120]	19	10	16	87	72	29	11	53	66	91	100
Isoleucine/Leucine[24]	17	100	70	83	85	52	36	96	85	70	61
Methionine[24,48,72,120]	27	61	54	61	46	28	18	93	100	62	55
Ornithine[24,48,96,120]	12	66	100	63	51	45	21	65	59	63	64
Phenylalanine[24]	100	84	93	65	59	65	20	64	66	51	52
Proline[24,48,96,120]	20	14	17	41	78	5	55	100	58	44	25
Serine[48,96,120]	22	62	54	57	44	45	72	100	69	60	61
Threonine[120]	36	44	45	85	96	68	86	100	90	74	29
Tryptophan[72,96,120]	75	33	26	43	36	30	24	62	92	100	66
Tyrosine[24,72,96,120]	28	38	36	66	49	38	10	55	88	100	95
Valine[24,96]	22	78	73	62	57	30	33	100	60	37	30

Superscript numbers indicates time points where significant difference to equivalent control point was observed (t-test, $P < 0.05$)

3.3. Amino acids analysis

The influence of TBT on 26 amino acids composition was examined with the use of LC-MS/MS technique and 23 of them were detected, whereas isoleucine and leucine could not be separated under the tested conditions. Cysteine, glycine and homocysteine were not detected. The LC-MS/MS data from control (c) and TBT-treated (TBT) samples were subjected to principal component analysis (PCA) with MarkerView™ software. PCA analysis showed the impact of TBT on the selected *C. echinulata* amino acids content. The main differences occurred during the first 48 h of the culture, as presented in Fig. 4, where the samples '0h', 'TBT24' and 'TBT48' are located on the chart at the longest mutual distances to each other and other samples. The analytes determining differences between the samples are located on the Pc1 loadings chart (Fig. 4). To examine all the data, the PCA loadings (peak areas) for each analyte were averaged and recalculated as relative percentage values (100% is the highest loading for each analyte). To facilitate data evaluation, a hit map and simple chart scoring were applied (Table 1). The most important differences were observed for the results obtained after 24 h and 48 h of incubation, where the fungus growth was strongly inhibited by TBT (Fig. 2).

Under stress conditions caused by TBT, the contents of 19 from 23 detected amino acids were affected in at least two consecutive time points, demonstrating that the xenobiotic caused a considerable impact on the fungus primary metabolism. During 24-48 h of the experiment aminoisobutyrate, alanine, asparagine, betaine, proline, serine and threonine were significantly upregulated in the TBT containing cultures (Table 1). Alanine and betaine showed a maximum relative concentration after 24 h of incubation in the

presence of TBT. Interestingly, accumulation of betaine was observed only after 24 h; afterwards, the relative concentration of betaine was maintained at a constant low level (Table 1). Significant downregulation after 24 h of incubation in the TBT presence was observed for arginine, dimethyl glycine, lysine, glutamine, histidine, isoleucine/leucine, methionine, ornithine, phenylalanine, tyrosine and valine (Table 1). However, after 48 h or later the amount of these amino acids in TBT-containing cultures increased and demonstrated even higher relative concentrations at the end of the experiment compared to the control samples (e.g. arginine, histidine or tyrosine). Except for 24 h cultures, only in the case of dimethyl glycine, isoleucine/leucine and phenylalanine, there were no significant differences between TBT-containing and control samples.

3.4. Protein analysis

A preliminary study of the TBT impact on the intracellular protein profile of the filamentous fungus was conducted for the first time. Based on the 1D SDS-PAGE analysis (Fig. 5), 22 protein bands from the TBT-containing sample and two intensive protein bands from the control culture (3 and 8) were taken for tryptic digestion followed by LC-MS/MS analysis. The homology (MASCOT searches) and functional alignments (BLAST searches with the use of delta-blast algorithm) of the 24 tested protein bands allowed for the identification and/or functional alignment of 15 protein bands, resulting in the final number of 20 identified proteins (Table 2). The tested organism was not sequenced; however, on the basis of sequence homology, it was revealed that the majority of the identified proteins belonged to the fungi from the *Mucorales* order, the same as the tested strain. In 1D electrophoresis one band often contains more than one protein; therefore, the conclusion concerning the role of identified proteins in the examined process was difficult. Only two protein bands (3K and 8K) were overexpressed in the control sample; the other protein bands had a higher intensity in the TBT-containing sample.

Identified proteins could be classified as involved in the ROS defence system (peroxiredoxin, nuclease C1), cell wall architecture (chitin deacetylase, UDP-glucose dehydrogenase), TCA cycle (malate dehydrogenase), sugar and energy-related systems (enolase and ATP synthase) and amino acids synthesis (5-methyltetrahydropteroyltriglutamate-homocysteine methyltransferase). The most conspicuous observation was strong overexpression of peroxiredoxin during TBT exposure. As showed in Fig. 5, peroxiredoxin had the most intensive band (no. 19) when compared to the other proteins. This difference is particularly evident in relation to control sample. An interesting result was obtained for the overexpression of nuclease C1 (bands 15 and 16) and malate dehydrogenase in TBT-treated sample.

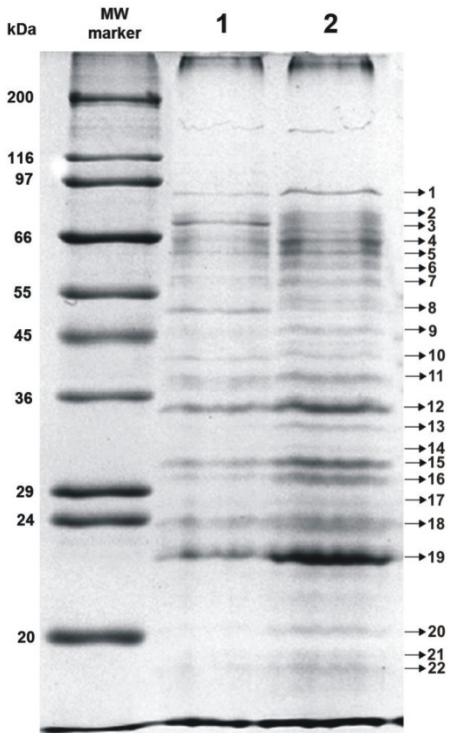

Fig. 5. 1-D SDS-PAGE analysis of the *C. echinulata* proteome in the absence (line 1) or presence of TBT (line 2).

4. Discussion

The major role in the elimination of xenobiotics from the environment is played by microorganisms (Gadd 2000; Desai 2010). Only one described fungal strain - *C. elegans* (Bernat et al. 2002), was capable of effectively eliminating high concentrations of TBT with DBT and MBT by-products formation. *C. echinulata* conducted TBT degradation on Sabouraud medium in a manner similar to *C. elegans*. In contrast to *C. elegans* which eliminated over 60% of TBT (5 mg l^{-1}) after 7 days of incubation (Bernat and Długoński 2002), *C. echinulata* degraded 91% of the xenobiotic after 5 days of culturing. In addition, the TBT biodegradation curve in *C. echinulata* (TBT

Table 2. Proteins identified by LC-MS/MS.

Band no[a]	Protein name[b]	Species homology	Accession no[c]	Score	Matched Sequence/ Unique Peptides	Sequence coverage	Delta-BLAST results	Fold change[d,e]
1	5-methyltetrahydropteroyltri-glutamate-homocysteine methyltransferase	*Lichtheimia corymbifera* JMRC:FSU:9682	A0A068SGC6_9FUNG	117	1/1	2%	[cd03312] CIMS - Cobalamine-independent methonine synthase, or MetE, N-terminal domain_like	2,2
2	hypothetical protein S7711_11496	*Stachybotrys chartarum* IBT 7711	A0A084AHD0_STACH	81	2/2	2%	[COG2051] Ribosomal protein S27E [Translation, ribosomal structure and biogenesis]	1,9
	TAT-binding protein-like protein 7	*Cryptococcus gattii* WM276	gi|317460266	74	2/2	3%	[pfam03941] Inner centromere protein, ARK binding region	
	Uncharacterized protein	*Mucor circinelloides* f. *circinelloides* (strain 1006PhL)	S2IZG8_MUCC1	77	2/2	3%	[cd00086] Homeodomain; DNA binding domains involved in the transcriptional regulation of key eukaryotic developmental processes	
3K	Uncharacterized protein	*Absidiaida hoensis* var. *thermophila*	A0A077WJ15_9FUNG	102	1/1	4%	[cd10952] Catalytic NodB homology domain of *Mucor rouxii* chitin deacetylase and similar proteins	1,3
	Chitin deacetylase	*Mucor circinelloides* f. *circinelloides* (strain 1006PhL)	S2JG56_MUCC1	83	1/1	4%		
3	Chitin deacetylase	*Amylomyces rouxii*	CDA_AMYRO	72	2/2	7%		
	Chitin deacetylase	*Mucor circinelloides* f. *circinelloides* (strain 1006PhL)	S2JG56_MUCC1	72	2/2	7%		
4	NOT IDENTIFIED							1,6
5	UDP-glucose dehydrogenase	*Lichtheimia corymbifera* JMRC:FSU:9682	A0A068SBD3_9FUNG	154	3/1	7%	[pfam03721] UDP-glucose/GDP-mannose dehydrogenase family, NAD binding domain	4,2
		Absidiaida hoensis var. *thermophila*	A0A077WFT0_9FUNG	154	3/1	7%	[cd00882] Rat sarcoma (Ras)-like superfamily of small	

							guanosine triphosphatases (GTPases). [pfam03721] UDP-glucose/GDP-mannose dehydrogenase family, NAD binding domain	
		Rhizopus delemar (strain RA 99-880 / ATCC MYA-4621 / FGSC 9543 / NRRL 43880)	I1BJF8_RHIO9	154	3/1	9%	[pfam00984] UDP-glucose/GDP-mannose dehydrogenase family, central domain	
6	NOT IDENTIFIED							7,3
7	V-type ATPase	*Lichtheimia corymbifera* JMRC:FSU:9682	gi|661185643	80	1/1	2%	[cd01135] V/A-type ATP synthase (non-catalytic) subunit B	1,8
	Putative ZYRO0C16984p	*Absidiaida hoensis* var. *thermophila*	gi|671690638	80	1/1	2%		
8K	Enolase	*Cunninghamella elegans*	ENO_CUNEL	512	8/5	28%	[cd03313] Enolase	1,9
	ATP synthase subunit beta	*Mucor circinelloides* f. *circinelloides* (strain 1006PhL)	S2IV94_MUCC1	248	6/3	17%	[cd01133] F1 ATP synthase beta subunit, nucleotide-binding domain	
	Putative ATP synthase subunit beta	*Rhizopus microsporus*	gi|729711200	245	6/4	17%		
8	ATP synthase subunit beta	*Mucor circinelloides* f. *circinelloides* (strain 1006PhL)	S2IV94_MUCC1	112	3/2	8%	[cd01133] F1 ATP synthase beta subunit, nucleotide-binding domain	
	Enolase	*Cunninghamella elegans*	ENO_CUNEL	92	2/2	8%	[cd03313] Enolase	
	Putative ATP synthase beta chain, mitochondrial	*Rhizopus microsporus*	gi|727144303	88	2/1	6%	[cd01133] F1 ATP synthase beta subunit, nucleotide-binding domain	
9	NOT IDENTIFIED							5,5
10	NOT IDENTIFIED							1,4
11	Putative Malate dehydrogenase	*Rhizopus microsporus*	gi|729714123	311	5/0	23%	[cd01337] Glyoxysomal and mitochondrial malate dehydrogenases	1,6
	malate dehydrogenase	*Rhizopus delemar* (strain RA 99-880 / ATCC MYA-4621 / FGSC 9543 / NRRL 43880)	I1BQQ7_RHIO9	296	4/0	16%		
	malate dehydrogenase	*Mucor circinelloides* f. *circinelloides* (strain 1006PhL)	S2J7L6_MUCC1	291	5/0	23%		
12	malate dehydrogenase	*Paracoccidioides lutzii* (strain ATCC MYA-826 / Pb01)	C1GNF8_PARBA	98	3/2	11%	[cd01337] Glyoxysomal and mitochondrial malate dehydrogenases	2,6
	malate dehydrogenase	*Paracoccidioides brasiliensis*	Q7ZA65_PARBR	98	3/2	11%		
	Transaldolase	*Rhizopus delemar* (strain RA 99-880 / ATCC MYA-4621 / FGSC 9543 / NRRL 43880)	I1CEK5_RHIO9	93	2/2	7%	[cd00957] Transaldolases including both TalA and TalB	
13	NOT IDENTIFIED							7,2
14	NOT IDENTIFIED							TBT
15	Nuclease C1	*Cunninghamella echinulata* var *echinulata*	NUC1_CUNEE	206	4/4	19%	[cd00091] DNA/RNA non-specific endonuclease	3,0
	Minor nuclease C1B isoform	*Cunninghamella echinulata* var. *echinulata*	Q9UUS3_CUNEE	206	4/4	18%		
	Voltage-dependent ion-selective channel	*Lichtheimia corymbifera* JMRC:FSU:9682	A0A068RIS3_9FUNG	88	2/2	7%	[cd07306] Voltage-dependent anion channel of the outer mitochondrial membrane	
16	Minor nuclease C1B isoform	*Cunninghamella echinulata* var. *echinulata*	Q9UUS3_CUNEE	515	11/11	44%	[cd00091] DNA/RNA non-specific endonuclease	4,4
	Nuclease C1	*Cunninghamella echinulata* var. *echinulata*	gi|3914183	409	8/8	36%		
	Elongation factor 1-beta	*Cladophialophora yegresii* CBS 114405	W9VTJ9_9EURO	61	1/1	5%	[cd00292] Elongation factor 1 beta (EF1B) guanine nucleotide exchange domain	
17	hypothetical protein RMATCC62417_06621	*Rhizopus microsporus*	gi|727147104	104	2/2	6%	[pfam00450] Serine carboxypeptidase	TBT
	Putative Rho-gdp dissociation inhibitor	*Rhizopus microsporus*	gi|727153664	71	2/2	21%	[pfam02115] RHO protein GDP dissociation inhibitor	
18	NOT IDENTIFIED							2,1
19	peroxiredoxin 1	*Lichtheimia corymbifera* JMRC:FSU:9682	gi|661185649	87	2/1	13%	[cd03015] Peroxiredoxin (PRX) family	3,1
	Putative Peroxiredoxin	*Absidiaida hoensis* var. *thermophila*	gi|671690634	87	2/1	13%		
	Peroxiredoxin	*Mucor circinelloides* f. *circinelloides* (strain 1006PhL)	S2K2B6_MUCC1	84	2/1	12%		
20	Pc22g23680 protein	*Penicillium chrysogenum* (strain ATCC 28089 / DSM 1075 / Wisconsin 54-1255)	B6HW37_PENCW	63	1/1	8%	[pfam12680] SnoaL-like domain;This family contains a large number of proteins that share the SnoaL fold	5,6
21	NOT IDENTIFIED							3,4
22	NOT IDENTIFIED							2,8

[a] Bands 3K and 8K were from the control sample. [b] Maximum of three best proteins with the highest score were presented. [c] If a protein was identified using both databases, the accession for the protein with the highest score was described. [d]Fold change was calculated as a ratio of the intensity of the protein bands between the control sample and the TBT-containing sample. [e]TBT means that protein band was present only in the sample from the TBT-incubated culture.

concentration 5 mg l^{-1}) was similar to that in *C. elegans* (TBT concentration 10 mg l^{-1} of TBT) (Bernat and Długoński 2002, 2007). The first significant amount of DBT and MBT observed on 3rd day of the culture as well as the general biodegradation process in the tested *Cunninghamella* species were closely related to the microorganisms growth. The ability of *Cunninghamella* sp. to biotransform a wide range of xenobiotics and drugs using both phase I and phase II mechanisms is well-known due to the similarity to the mammalian metabolism (Asha and Vidyavathi 2009; Murphy 2015). Therefore, a search for other TBT by-products was performed. LightSight™ is a useful tool in the development of methods applied for the metabolites of phase I or II screening. The software analyses the data by comparing the test sample against the control sample, followed by the generation of a list of probable

metabolite hits (Ramirez-Molina et al. 2009; Song et al. 2014). Except DBT and MBT, only hydroxylated TBT (TBTOH) was detected. Interestingly, the hydroxyl group was bound directly to a tin atom. This type of TBT hydroxylation has not been postulated in a biological system although hydroxylated intermediates formed during TBT degradation had been reported previously (Matsuda et al. 1993; Bernat et al. 2013). The process of TBT elimination was accompanied by cytochrome P450 activity (Bernat and Długoński 2002; Ohhira et al. 2006). The comparison of the obtained mass spectra with the one presented by Bekri et al. (2006) and Bernat et al. (2013) confirmed that the detected compound was a novel tin-hydroxylated TBT**.** Taking into account the results obtained for *C. elegans* and *C. echinulata*, the formation of DBT, MBT and hydroxylated intermediates seems to be an integral part of TBT removal by fungi belonging to the *Cunninghamella* genus.

ROS cause several negative effects on both, the structure and the cellular metabolism (Circu and Aw 2010), therefore organisms developed a number of enzymatic and non-enzymatic antioxidant mechanisms. The majority of the mechanisms of ROS defence systems involve various kinds of reactive oxygen scavenging redox reactions. These reactions may be catalysed by stress response enzymes or be a result of the chemical and biochemical pathways incorporating various compounds, which leads to the modulation of the intracellular redox environment. Biodegradation of TBT by *C. echinulata* presented in this work occurs effectively on the rich Sabouraud medium as an oxygen-related metabolic pathway. The time courses of the TBT elimination and formation of biodegradation intermediates - DBT, MBT and TBTOH reflects the changes in the mycelium growth as well as in the examined proteins and selected amino acids. In TBT-containing cultures a significant upregulation of peroxiredoxin (band 19) and nuclease C1 (band 15 and 16) (Fig. 5, Table 2) and an increased contents of aminoisobutyrate, alanine, betaine and proline (Table 1) supports the fact that ROS were generated during the xenobiotic biodegradation.

Peroxiredoxins are important antioxidant enzymes found in organisms from all kingdoms. This group of enzymes are mainly involved in cellular response against oxidative damage by reducing hydrogen peroxide (Rhee 2001). Previous studies had focused on the study of the activity of the other antioxidant enzymes, such as SOD or CAT rather than peroxiredoxin participation in the regulation of oxidative stress in organisms exposed to TBT. Jia et al. (2009) examined the level of the activity of selected enzymatic antioxidants in TBT-treated abalone *Haliotis diversicolor supertexta*. Exposure to TBT (0.35 μg Sn l^{-1}) caused changes in the acidic (ACP) and alkaline (AKP) phosphatase activity in abalone hepatopancreas and hemolymph. Thus, SOD and CAT do not seem to be involved in the TBT detoxification process in *H. diversicolor supertexta* hepatopancreas. On the other hand, the study conducted by Zhou et al. (2010) on the same research model showed a decreased SOD activity and increased peroxidase activity in abalone heamolymph. Thus, the obtained results suggest that peroxiredoxin should be taken into account as an important ROS scavenger in TBT exposed organisms. The increased expression of peroxiredoxin may also be caused by a high concentration of DBT after 5 days of incubation (Fig. 1C) due to the fact, that DBT also induces oxidative stress (Chantong et al. 2014). An interesting result was obtained for nuclease C1 – highly upregulated in a TBT-containing sample. Nuclease C1 in *C. echinulata* was described by Ho et al. (1998) and showed a significant similarity to the sequence of the mitochondrial nucleases of *Saccharomyces cerevisiae* (44% identity) and *Schisosaccharomyces pombe* (42% identity). However, its role in the fungal cells remains ambiguous as the enzyme has a complex nature. Additionally, *Cunninghamella* sp. were not sequenced, and the reported nuclease was described only once. The DELTA-BLAST search conducted on band 15 digest confirmed that the protein is a member of the NUC superfamily. The nuclease from *C. echinulata* showed a similarity to the endonuclease G from *Rhizopus micrococcus* (57% identity) and mitochondrial endonuclease G from *Mucor circinelloides* f. *circinelloides* 1006PhL (57% identity), in contrast to Nuc1p from *S. cerevisiae* (45% identity) (Marchler et al. 2015). Endonuclease G is a mitochondrial nuclease employed in life and death processes in the cell (Büttner et al. 2007). Moreover, it was involved in the nucleosomal DNA fragmentation under oxidative stress in rat primary hepatocytes (Ishihara and Shimamoto 2006). Considering the fact that TBT induced DNA damage (Liu et al. 2006; Morales et al. 2013), the overexpression of this enzyme points it as a possible DNA protector in the examined process.

Mitochondria are key structures involved in several cellular mechanisms. TBT is known to disrupt the mitochondrial functions, especially related with the respiratory chain (Nesci et al. 2011). The downregulation of ATP synthase in the presence of TBT confirmed the negative effect of the compound on mitochondria. Moreover, TCA cycle components located in this organella are correlated with many metabolic pathways occurring in the cell. Enolase and malate dehydrogenase are involved in sugar and energy-related metabolism and they down- and upregulation, respectively, suggest a varied disrupting action on the cell metabolism. The disorders in metabolism caused by TBT were showed in bacteria and abalone (Cruz et al. 2010; Zhou et al. 2010). Methionine synthases are enzymes that catalyse the formation of methionine from homocysteine. Thus, the upregulated 5-methyltetrahydropteroyltriglutamate-homocysteine methyltransferase (band 1) and an increased level of methionine seem to be responsible for the accumulation of methionine in fungal cells (Table 1). It was proved, that methionine accumulation exhibits cytoprotective and antioxidant properties in living cells (Bender et al. 2008). Because the highest level for methionine was observed in 48 and 72 h of the culture, it can be assumed that the level of expression of the methionine synthase was higher at earlier stages implying a high concentration of methionine in this stage of the culture. Chitin deacetylase and UDP-glucose dehydrogenase are involved in cell wall biosynthesis. The observed changes in the hyphae structure and membrane lipid composition in *C. elegans* during the exposure to TBT (Bernat and Długoński 2012; Bernat et al. 2009b; 2014a) can indicate a role of these enzymes in the TBT induced modification of cell membranes.

The second antioxidant strategy examined in this work involved free amino acids analysis. TBT-related stress induced changes in the relative concentration of selected amino acids, whose accumulation is a known marker of the defence mechanism towards ROS. However, the impact of stress conditions on fungal amino acids composition is still poorly understood. In a *C. echinulata* TBT-treated culture, significant changes in the amount of 19 from 23 detected free amino acids were observed in a time-dependent way. Some of them showed maximum amount after 24 h, 48 h or at the later time points. Proline and betaine are many the most important organic compounds accumulated in a variety of organisms in response to oxidative stress (Ashrad and Foolad 2007; Liu et al. 2011). Particularly proline is the object of an intense study, showing its broad influence on the physiology of the cells under stress, which is not limited only to osmoregulation but also enables the removal of reactive oxygen species or stabilization of the cell membranes (Takagi et al. 2008). In the examined fungal cultures the relative concentration of proline and betaine were significantly increased during the exposure to the xenobiotic. The study conducted by Zhou et al. (2010) revealed disturbances in the metabolism of abalone (*Haliotis diversicolor supertexta*) during the exposure to TBT. Incubation with the xenobiotic showed increased levels of alanine and glutamine as well as the other kinds of compounds such as: lactate, acetate, and succinate. A decreased level in concentrations of TCA cycle compounds pyruvate and glucose was also observed. Another example of an amino acid linked with oxidative stress is aminoisobutyric acid (Mimura et al. 1994). Similar trends for alanine and aminoisobutyrate and glutamine were observed in *C. echinulata* in TBT-treated samples.

5. Conclusions

C. echinulata was capable of effective TBT biodegradation during 5 days of culture. The TBT hydroxylation directly on a tin atom has been described for the first time, and TBTOH appears to be a key intermediate that may be involved in the TBT debuthylation leading to DBT and MBT formation. However, the exposure to the biocide was a stress factor for the fungus manifested by a strong inhibition of growth at the initial stages of the culture. In the presented study the microorganism strategy against TBT-induced stress was examined on the protein and amino acids level. Proteomics analysis showed changes in the protein profile, especially related with the antioxidant defence mechanism (peroxiredoxin and nuclease). Significant changes in most of the analysed free amino acids were also observed, especially the accumulation of oxidative stress markers such as aminoisobutyrate, betaine and proline. The obtained data proved that during TBT biodegradation oxidative stress occurred. A deeper explanation of TBT impact on the fungus metabolism requires further investigation incorporating comparative proteomics as well as broader targeted metabolomics.

6. Acknowledgements

The authors are grateful to Dr P. Bernat, University of Łódź, for help with the sample preparation for the organotins analysis and discussion of the obtained results. The study was supported by the National Science Centre, Poland (Project No. UMO-2014/13/N/NZ9/00878).

7. References

Antizar-Ladislao, B., 2008. Environmental levels, toxicity and human exposure to tributyltin (TBT)-contaminated marine environment. A review. Environ. Int. 34, 292-308.

Asha, S., Vidyavathi, M., 2009. *Cunninghamella*. A microbial model for drug metabolism studies–A review. Biotechnol. Adv. 27, 16-29.

Ashraf, M., Foolad, M., 2007. Roles of glycine betaine and proline in improving plant abiotic stress resistance. Environ. Exp. Bot. 59, 206-216.

Banoub, J. H., Miller-Banoub, J., Sheppard, G. V., Hodder, H. J., 2004. Electrospray tandem mass spectrometric measurements of organotin compounds. J. of Spectro. 18, 95-112.

Baxter, C. J., Redestig, H., Schauer, N., Repsilber, D., Patil, K. R., Nielsen, J., Selbig, J., Liu, J., Fernie, A. R., Sweetlove, L. J., 2007. The metabolic response of heterotrophic Arabidopsis cells to oxidative stress. Plant Physiol. 143, 312-325.

Békri, K., Saint-Louis, R., Pelletier, E., 2006. Determination of tributyltin and 4-hydroxybutyldibutyltin chlorides in seawater by liquid chromatography with atmospheric pressure chemical ionization-mass spectrometry. Anal. Chim. Acta 578, 203-212.

Bender, A., Hajieva, P., Moosmann, B., 2008. Adaptive antioxidant methionine accumulation in respiratory chain complexes explains the use of a deviant genetic code in mitochondria. Proc. Natl. Acad. Sci. U.S.A. 105, 16496-16501.

Bernat, P., Długoński, J., 2002. Degradation of tributyltin by the filamentous fungus *Cunninghamella elegans*, with involvement of cytochrome P-450. Biotechnol. Lett. 24, 1971-1974.

Bernat, P., Długoński, J., 2007. Tributyltin chloride interactions with fatty acids composition and degradation ability of the filamentous fungus *Cunninghamella elegans*. Int. Biodeterior. Biodegrad. 60, 133-136.

Bernat, P., Długoński, J., 2009a. Isolation of *Streptomyces* sp. strain capable of butyltin compounds degradation with high efficiency. J. Hazard. Mater. 171, 660-664.

Bernat, P., Słaba, M., Długoński, J., 2009b. Action of tributyltin (TBT) on the lipid content and potassium retention in the organotins degradating fungus *Cunninghamella elegans*. Curr. Microbiol. 59, 315-320.

Bernat, P., Długoński, J., 2012. Comparative study of fatty acids composition during cortexolone hydroxylation and tributyltin chloride (TBT) degradation in the filamentous fungus *Cunninghamella elegans*. Int. Biodeterior. Biodegrad. 74, 1-6.

Bernat, P., Szewczyk, R., Krupiński, M., Długoński, J., 2013. Butyltins degradation by *Cunninghamella elegans* and *Cochliobolus lunatus* co-culture. J. Hazard. Mater. 246, 277-282.

Bernat, P., Gajewska, E., Szewczyk, R., Słaba, M., Długoński, J., 2014a. Tributyltin (TBT) induces oxidative stress and modifies lipid profile in the filamentous fungus *Cunninghamella elegans*. Environ. Sci. Pollut. R. 21, 4228-4235.

Bernat, P., Siewiera, P., Soboń, A., Długoński, J., 2014b. Phospholipids and protein adaptation of *Pseudomonas* sp. to the xenoestrogen tributyltin chloride (TBT). World J. Microbiol. Biotechnol. 30, 2343-2350.

Bundy, J. G., Davey, M. P., Viant, M. R., 2009. Environmental metabolomics: a critical review and future perspectives. Metabolomics 5, 3-21.

Büttner, S., Eisenberg, T., Carmona-Gutierrez, D., Ruli, D., Knauer, H., Ruckenstuhl, C., Sigrist, C., Wissing, S., Kollroser, M., Frohlich, K., Sigrist, S., Madeo, F., 2007. Endonuclease G regulates budding yeast life and death. Mol. Cell. 25, 233-246.

Chantong, B., Kratschmar, D. V., Lister, A., Odermatt, A., 2014. Dibutyltin promotes oxidative stress and increases inflammatory mediators in BV-2 microglia cells. Toxicol. lett. 230, 177-187.

Circu, M. L., Aw, T. Y., 2010. Reactive oxygen species, cellular redox systems, and apoptosis. Free Radical Biol. Med. 48, 749-762.

Cruz, A., Caetano, T., Suzuki, S., Mendo, S., 2007. *Aeromonas veronii*, a tributyltin (TBT)-degrading bacterium isolated from an estuarine environment, Ria de Aveiro in Portugal. Mar. Environ. Res. 64, 639-650.

Cruz, A., Oliveira, V., Baptista, I., Almeida, A., Cunha, Â., Suzuki, S., Mendo, S., 2012. Effect of tributyltin (TBT) in the metabolic activity of TBT-resistant and sensitive estuarine bacteria. Environ. Toxicol. 27, 11-17.

Cruz, A., Anselmo, A. M., Suzuki, S., Mendo, S., 2015. Tributyltin (TBT): a review on microbial resistance and degradation. Crit. Rev. Env. Sci. Technol. 45, 970-1006.

Das, K., Roychoudhury, A., 2014. Reactive oxygen species (ROS) and response of antioxidants as ROS-scavengers during environmental stress in plants. Front. Environ. Sci. 2, 53.

Desai, C., Pathak, H., Madamwar, D., 2010. Advances in molecular and "-omics" technologies to gauge microbial communities and bioremediation at xenobiotic/anthropogen contaminated sites. Bioresour. Technol. 101, 1558-1569.

Gadd, G. M., 2000. Microbial interactions with tributyltin compounds: detoxification, accumulation, and environmental fate. Sci. Total Environ. 258, 119-127.

Gupta, M., Dwivedi, U. N., Khandelwal, S., 2011. C-Phycocyanin: an effective protective agent against thymic atrophy by tributyltin. Toxicol. lett. 204, 2-11.

Ho, H. C., Shiau, P. F., Liu, F. C., Chung, J. G., Chen, L. Y., 1998. Purification, characterization and complete amino acid sequence of nuclease CI from *Cunninghamella echinulata* var. *echinulata*. Eur. J. Biochem. 256, 112-118.

Ishihara, Y., Kawami, T., Ishida, A., Yamazaki, T., 2012. Tributyltin induces oxidative stress and neuronal injury by inhibiting glutathione S-transferase in rat organotypic hippocampal slice cultures. Neurochem. Int. 60, 782-790.

Ishihara, Y., Shimamoto, N., 2006. Involvement of endonuclease G in nucleosomal DNA fragmentation under sustained endogenous oxidative stress. J. Biol. Chem. 281, 6726-6733.

Jia, X., Zhang, Z., Wang, S., Lin, P., Zou, Z., Huang, B., Wang, Y., 2009. Effects of tributyltin (TBT) on enzyme activity and oxidative stress in hepatopancreas and hemolymph of small abalone, *Haliotis diversicolor supertexta*. Chin. J. Oceanol. Limnol. 27, 816-824.

Kroll, K., Pähtz, V., Kniemeyer, O., 2014. Elucidating the fungal stress response by proteomics. J. Proteomics 97, 151-163.

Liu, H. G., Wang, Y., Lian, L., Xu, L. H., 2006. Tributyltin induces DNA damage as well as oxidative damage in rats. Environ. Toxicol. 21, 166-171.

Liu, J., Wisniewski, M., Droby, S., Vero, S., Tian, S., Hershkovitz, V., 2011. Glycine betaine improves oxidative stress tolerance and biocontrol efficacy of the antagonistic yeast *Cystofilobasidium infirmominiatum*. Int. J. Food Microbiol. 146, 76-83.

Marchler-Bauer, A., Derbyshire, M.K., Gonzales, N.R., Lu, S., Chitsaz, F., Geer, L.Y., Geer, R.C., He, J., Gwadz, M., Hurwitz, D.I., Lanczycki, C.J., Lu, F., Marchler, G.H., Song, J.S., Thanki, N., Wang, Z., Yamashita, R.A., Zhang, D., Zheng, C., Bryant, S.H., 2015. CDD: NCBI's conserved domain database. Nucleic Acids Res. 43, 222-226.

Matsuda, R., Suzuki, T., Saito, Y., 1993. Metabolism of tri-n-butyltin chloride in male rats. J. Agric. Food. Chem. 41, 489-495.

Mimura, H., Nagata, S., Matsumoto, T., 1994. Concentrations and compositions of internal free amino acids in a halotolerant *Brevibacterium* sp. in response to salt stress. Biosci. Biotechnol. Biochem 58, 1873-1874.

Morales, M., Martínez-Paz, P., Ozáez, I., Martínez-Guitarte, J. L., Morcillo, G., 2013. DNA damage and transcriptional changes induced by tributyltin (TBT) after short in vivo exposures of *Chironomus riparius* (Diptera) larvae. Comp. Biochem. Physiol. C-Toxicol. Pharmacol. 158, 57-63.

Murphy, C.D., 2015. Drug metabolism in microorganisms. Biotechnol. Lett. 37, 19-28.

Nesci, S., Ventrella, V., Trombetti, F., Pirini, M., Borgatti, A. R., Pagliarani, A., 2011. Tributyltin (TBT) and dibutyltin (DBT) differently inhibit the mitochondrial Mg-ATPase activity in mussel digestive gland. Toxicol. in Vitro 25, 117-124.

Ohhira, S., Enomoto, M., Matsui, H., 2006. Sex difference in the principal cytochrome P-450 for tributyltin metabolism in rats. Toxicol. Appl. Pharmacol. 210, 32-38.

QuEChERS-A Mini-Multiresidue Method for the Analysis of Pesticide Residues in Low-Fat Products, protocol available online at http://quechers.cvua-stuttgart.de.

Ramírez-Molina, C., Burton, L., 2009. Screening strategy for the rapid detection of *in vitro* generated glutathione conjugates using high-performance liquid chromatography and low-resolution mass spectrometry in combination with LightSight® software for data processing. Rapid Commun. Mass Spectrom. 23, 3501-3512.

Rhee, S. G., Kang, S. W., Chang, T. S., Jeong, W., Kim, K., 2001. Peroxiredoxin, a novel family of peroxidases. IUBMB life 52, 35-42.

Shevchenko, A., Tomas, H., Havli, J., Olsen, J. V., Mann, M., 2006. In-gel digestion for mass spectrometric characterization of proteins and proteomes. Nat. Protoc. 1, 2856-2860.

Song, Y. L., Jing, W. H., Yan, R., Wang, Y. T., 2014. Metabolic characterization of (±)-praeruptorin A *in vitro* and *in vivo* by high performance liquid chromatography coupled with hybrid triple quadrupole-linear ion trap mass spectrometry and time-of-flight mass spectrometry. J. Pharm. Biomed. Anal. 90, 98-110.

Szewczyk, R., Soboń, A., Różalska, S., Dzitko, K., Waidelich, D., Długoński, J., 2014. Intracellular proteome expression during 4-*n*-nonylphenol biodegradation by the filamentous fungus *Metarhizium robertsii*. Int. Biodeterior. Biodegrad. 93, 44-53.

Szewczyk, R., Soboń, A., Słaba, M., Długoński, J., 2015. Mechanism study of alachlor biodegradation by *Paecilomyces marquandii* with proteomic and metabolomic methods. J. Hazard. Mater. 291, 52-64.

Tabb, M. M., Blumberg, B., 2006. New modes of action for endocrine-disrupting chemicals. Mol. Endocrinol. 20, 475-482.

Takagi, H. 2008. Proline as a stress protectant in yeast: physiological functions, metabolic regulations, and biotechnological applications. Appl. Microbiol. Biotechnol. 81, 211-223.

Wei, R., Li, G., Seymour, A. B., 2010. High-throughput and multiplexed LC/MS/MRM method for targeted metabolomics. Anal. Chem. 82, 5527-5533.

Zhou, J., Zhu, X. S., Cai, Z. H., 2010. Tributyltin toxicity in abalone (*Haliotis diversicolor supertexta*) assessed by antioxidant enzyme activity, metabolic response, and histopathology. J. Hazard. Mater. 183, 428-43

SUPPORTING MATERIAL

Table S-1. Multiple reaction monitoring (MRM) MS/MS scan mode – compound dependant parameters applied in the screening method.

Q1 mass (Da)	Q3 Mass (Da)	Dwell time (ms)	Amino acid	DP (V)	EP (V)	CE (V)	CXP (V)
90	44	5	Alanine	25	10	17	10
104.1	87	5	Aminoisobutyrate	30	10	17	10
175.1	70	5	Arginine	25	10	32	10
133.1	74	5	Asparagine	30	10	23	10
134.	74	5	Aspartate	25	10	21	10
118.1	58	5	Betaine	40	10	41	10
122	76	5	Cysteine	25	10	20	10
104.1	58	5	Dimethyl glycine	30	10	20	10
148.1	84	5	Glutamate	25	10	23	10
147.1	84	5	Glutamine/Lysine	25	10	25	10
76	30.2	5	Glycine	20	10	21	10
156.1	110	5	Histidine	25	10	21	10
136	90	5	Homocysteine	50	10	20	10
132.1	86.2	5	Hydroxyproline/Isoleucine/Leucine	50	10	18	10
150.1	61	5	Methionine	40	10	31	10
133.1	70	5	Ornithine	40	10	30	10
166.1	120.2	5	Phenylalanine	50	10	19	10
116.1	70	5	Proline	50	10	20	10
106.0	60	5	Serine	25	10	18	10
120.1	102	5	Threonine	30	10	10	10
205.1	188.3	5	Tryptophan	25	10	16	10
182.1	136.3	5	Tyrosine	25	10	19	10
118.1	72	5	Valine	25	10	18	10